

Title	Six-fold rotationally symmetric vanadium oxide nanostructures by a morphotropic phase transition
Authors	O'Dwyer, Colm;Lavayen, Vladimir;Fuenzalida, David;Newcomb, Simon B.;Santa-Ana, María A.;Benevente, Englantina;Gonzalez, Guillermo;Torres, C. M. Sotomayor
Publication date	2007-11-12
Original Citation	O'Dwyer, C., Lavayen, V., Fuenzalida, D., Newcomb, S. B., Santa Ana, M. A., Benavente, E., Gonzalez, G. and Torres, C. M. Sotomayor (2007) 'Six#fold rotationally symmetric vanadium oxide nanostructures by a morphotropic phase transition', Physica Status Solidi (b), 244(11), pp. 4157-4160. doi: 0.1002/pssb.200776123
Type of publication	Article (peer-reviewed)
Link to publisher's version	https://onlinelibrary.wiley.com/doi/abs/10.1002/pssb.200776123 - 10.1002/pssb.200776123
Rights	© 2007 WILEY-VCH Verlag GmbH & Co. KGaA, Weinheim. This is the peer reviewed version of the following article: O'Dwyer, C. et al. (2007), Six#fold rotationally symmetric vanadium oxide nanostructures by a morphotropic phase transition. phys. stat. sol. (b), 244: 4157-4160, which has been published in final form at https://doi.org/10.1002/pssb.200776123 . This article may be used for non-commercial purposes in accordance with Wiley Terms and Conditions for Self-Archiving.
Download date	2023-09-25 00:16:55
Item downloaded from	https://hdl.handle.net/10468/6301



UCC

University College Cork, Ireland
Coláiste na hOllscoile Corcaigh

Six-Fold Rotationally Symmetric Vanadium Oxide Nanostructures by a Morphotropic Phase Transition

C. O'Dwyer^{*1}, V. Lavayen^{1,2}, D. Fuenzalida^{2,3}, S. B. Newcomb⁴, M. A. Santa Ana¹, E. Benavente³, G. González², and C. M. Sotomayor Torres¹

¹ Tyndall National Institute, University College Cork, Lee Maltings, Cork, Ireland

² Departamento de Química, Facultad de Ciencias, Universidad de Chile, Santiago, Chile

³ Department of Chemistry, Universidad Tecnológica Metropolitana, Santiago, Chile

⁴ Glebe Scientific Ltd., Newport, Co. Tipperary, Ireland

Received ZZZ, revised ZZZ, accepted ZZZ

Published online ZZZ

PACS 61.10.Nz; 61.14.Lj; 61.50.-f; 68.37.Hk; 81.20.-n; 81.30.-t

In this work, we report the first observation of unique hierarchical six-fold rotational symmetrical vanadium oxide based nanocomposite synthesized by a simple chemical route and highlight the first observation of a morphotropic reconstructive phase transition from a lamellar V_2O_5 to that of a single crystalline V_6O_{11} nanostructure.

copyright line will be provided by the publisher

1 Introduction

Considerable attention is now being directed to transition metal nanostructures, such as VO_x and ZnO , for example [1], based on their metal oxides [2,3] which, due to their versatile chemical properties often modulable by changes in the oxidation state of the metal coordination sphere, may lead to a variety of products and tunable materials [4,5]. From the laminar V_2O_5 xerogel [6], numerous two dimensional organic-inorganic intercalation products have been obtained [7].

In this report of unique hierarchical six-fold rotational symmetrical vanadium oxide based nanocomposite synthesized by a simple chemical route, structures were realised without the use of a catalyst. This method exploits the combination of surfactant/inorganic self-assembly process and host/guest intercalation chemistry to obtain anisotropic recrystallization of the vanadium oxide directly from its xerogel. A morphotropic reconstructive phase transition occurs during hydrothermal treatment rendering a V_6O_{11} single crystal nanostructure. Each nanostructure is composed of six spoke-like V_6O_{11} platelets of near-equal dimensions and crystal orientation. We examine the anisotropic 1D-3D structural evolution and elucidate the structural specifics of the shape-determining process.

2 Experimental

To synthesize the product, 5 ml of an aqueous solution of V_2O_5 xerogel (0.43×10^{-3} mol $V_2O_5 \cdot 1.5H_2O$) were treated with dodecanethiol by heating at 313 K for 2 h. After addition of 10 ml ethanol/ H_2O (1:1 v/v) the mixture was vigorously stirred for 48 h at 313 K. Approximately 3 ml of resulting dark green, gel-like suspension were then transferred to a Teflon-lined autoclave and heated under auto generated pressure at 453 K for several days. From obtained suspension a dark solid was separated, washed with water and ethanol and dried under vacuum (10^{-3} mm Hg) for 48 h. The final product corresponds to a 98.53% pure vanadate containing 1.34% dodecanethiol and 0.13% sulphur. Analysis calcu-

* Corresponding author: e-mail: codwyer@tyndall.ie, Phone: +353 21 4904391, Fax: +353 21 4904467

copyright line will be provided by the publisher

lated for $C_{0.15}H_{0.75}S_{0.02}O_{5.21}V_2$: C (0.955); H (0.346); S (0.34), Exp: C (0.956); H (0.396); S (0.347). After hydrothermal treatment, the resulting crystals are from the so-called vanadium Magnéli phases, defined by V_nO_{2n-1} ($3 \leq n \leq 9$) giving rise to a homologous series of compounds with closely related crystal structures where oxygen atoms form a distorted hexagonal-close-packed array [8].

The morphological characterization of the nanostructured products was performed by field emission scanning electron microscopy (FESEM) using a JEOL JSM-6700F operating at beam voltages between 1-10 kV. Electron transparent specimens were prepared by ion-milling techniques and placed on a holey carbon support. Transmission electron microscopy (TEM) and selected area electron diffraction (SAED) were conducted using a JEOL 2000FX operating at 200 kV.

3 Results and discussion

The morphology of the samples was studied using FESEM. The characteristic cog-like architecture of the as-synthesized structures is clearly shown in Fig. 1a. We observe a high degree of relative uniformity for each of the structures in the synthesized product, and quantities of several grammes are easily obtained from the synthesis procedure. Each structures has an average size of $1.5 \mu\text{m}$ where the diameter of the central core is $\sim 500 \text{ nm}$ and the length of each platelet measured from the outer edge of the core is also $\sim 500 \text{ nm}$. More detailed studies of the structural dimensions were provided by TEM. A typical region of the sample is shown at relatively low magnification in Fig. 1b where an individual nanostructure is observed. Each structure exhibits three axes of symmetry and contains the six platelets marked at A-F that protrude from the central axis. The $\sim 60^\circ$ angle between each pair of platelets corresponds to six-fold rotational symmetry in the c plane. It should be noted that the relatively high thickness of the branches forming the platelet A, for example, arises from the fact that the particle is lying at an angle to the incident electron beam. Selected area electron diffraction measurements in Figs 1 and 2 confirm the single-crystalline V_6O_{11} phase of the nanostructures with reconstructed lattice parameters of $a_0 = 0.544 \text{ nm}$, $b_0 = 0.699 \text{ nm}$ and $c_0 = 2.366 \text{ nm}$; Space Group = P-1.

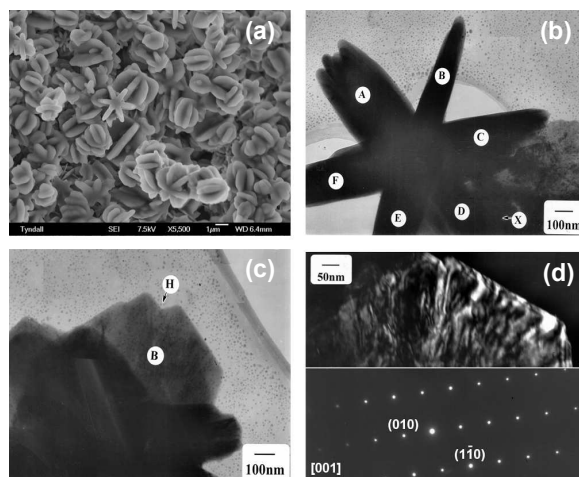


Fig. 1 (a) FESEM micrograph of the as-synthesized nanostructures. (b) TEM image of an individual structure with the six platelets labelled A-F. (c) TEM image of a single platelet after tilting (b) in the direction marked X. (d) SAED pattern of an individual platelet along its $[-7,9-1]$ zone normal of the (001) face of V_6O_{11} .

The diffraction pattern of the resulting material is shown in Fig. 2a and is consistent with the intercalation of the thiol into the lamellar matrix (an FESEM image of which is shown inset), and indicates that the framework of the host is preserved, coherent with a topotactic reaction. The presence of the thiol contribution within the lamellar nanostructure is clearly discernible by comparison with its monolayer diffraction pattern.

copyright line will be provided by the publisher

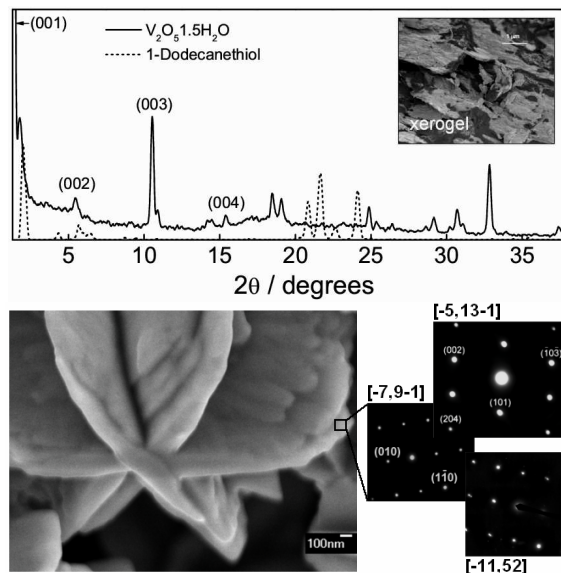
1
2
3
4
5
6
7
8
9
10
11
12
13
14
15
16
17
18
19
20
21
22
23
24
25
26
27
28
29
30
31
32
33
34
35
36
37
38
39
40
41
42
43
44
45
46
47
48
49
50
51
52

Fig. 2 (a) XRD pattern of both the $V_2O_5 \cdot 1.5H_2O$ xerogel and of a grazing-incidence pattern of a dodecanethiol monolayer (*inset*) FESEM image of the lamellar xerogel (b) FESEM micrograph of an as-synthesized nanostructure. The corresponding SAED patterns (*right*) of an individual platelet along its $[-5,3-11]$, $[-7,9-1]$, and $[-11,52]$ zone normals of the V_6O_{11} phase.

We also observe that this product exhibits a lamellar structure with an interlamellar distance measured to be 0.25 nm, corresponding to one monolayer of dodecanethiol intercalated between the xerogel lamella (interlamellar distance 0.127 nm). There is a notable absence of a high intensity (002) reflection from the xerogel, consistent with its arrangement as a bi-layered product where two vanadate layers are bound by surfactant [9] and this arrangement is stacked periodically back-to-back. Each of the structures consists of a central axis and each axis consists of spokes or platelets that self-assemble into a six-branched structure, as observed in Fig. 3. The platelets homogeneously distribute around the central axis, forming the rotationally symmetric architecture. The angle between each pair of adjacent branches is very close to 60° (Fig. 3b). The platelets are grown along the direction perpendicular to the central axis.

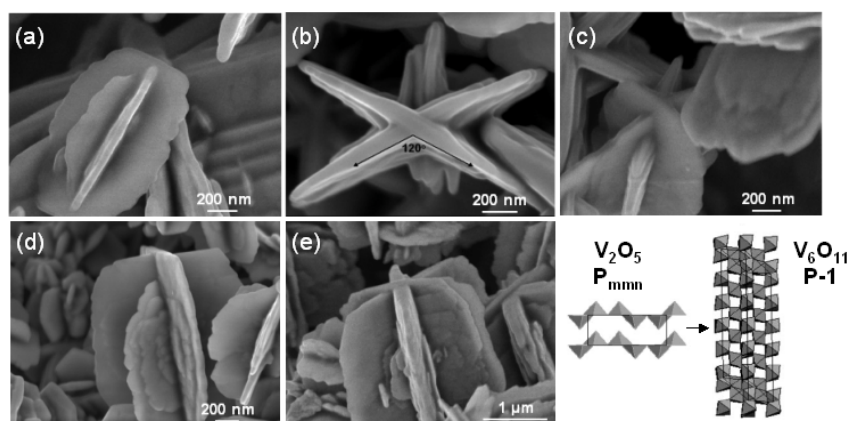


Fig. 3 (a-e) FESEM images of the nucleation of lamellar order and subsequent growth stages of the V_6O_{11} nanostructures (f) schematic difference between V_2O_5 (SG = P_{mnm}) and V_6O_{11} (SG = $P-1$) unit cell structures- constructed with VO_5 units.

1 The $V_2O_5 \cdot 1.5H_2O$ xerogel is essentially a stack of ribbon-like slabs, which are bi-layers of single V_2O_5
2 layers consisting of square pyramidal VO_5 units, as depicted in Fig. 3f. These 2D sheets are weakly
3 bound by van der Waals forces and are readily propped open by intercalation species such as do-
4 decanethiol in this instance. Hydrothermal treatment of the thiol-containing xerogel above 450 K induces
5 loss of bound water molecules and recrystallization of the material during thiol-bond weakening. After
6 the determination of a preferred crystalline phase during the initial nucleation stage from the xerogel, the
7 subsequent kinetic growth governs the final architecture of the nanocrystals. Figures 3a-e highlight the
8 principal stages of growth of the structures and evidence their six-fold rotational symmetry, which nucle-
9 ates progressively. Lamellar rearrangement of the xerogel occurs, and subsequent growth is crystal-
10 lographically ordered. In the presence of expunged thiols, the resulting plates experience an attachment
11 process due to the capping ability of the surfactant. The surface energy of an individual plate is quite
12 high, with two exposed flat planes, and they tend to form an angle with each other to decrease the surface
13 energy by reducing exposed areas.

14 The platelets grow along the crystallographically equivalent a axes along the $\pm[1010]$, $\pm[0110]$, and
15 $\pm[1100]$ directions. The V_2O_5 xerogel undergoes a morphotropic transition to V_6O_{11} reminiscent of a
16 reconstructive phase transition [10] where all homologous series V_nO_{2n-1} and V_nO_{2n+1} phases can be ulti-
17 mately derived from a common disordered polytype hexagonal structure [11].
18

19 4 Conclusions

20 In summary, we have successfully synthesized single crystal V_6O_{11} nanostructures from the V_2O_5
21 xerogel and polymer hybrid nanocomposite. Detailed TEM analyses elucidated the unique single crystal
22 structure and six-fold rotational symmetry of the structures. On cooling, the fraction of disordered
23 sequences of layers in the vanadate xerogel reduce and the intrinsically faulted ordered regions tend to
24 coalesce. Thus, the V_2O_5 xerogel undergoes a morphotropic transition to V_6O_{11} . These types of
25 mechanistic studies may form the basis for controlling morphological geometries of a wide range of
26 nanocrystalline products. Our systematic study of growth parameters in conjunction with detailed
27 structural studies have provided an outline of the shape-evolution process and may be applied to the
28 growth of low-dimensional structures of other materials with layered structure.
29

30
31 **Acknowledgements** This material is based upon work supported by the Science Foundation Ireland under Grant
32 No. 02/IN.1/172. Support from FONDECYT Grants 1050344, 1030102, 7050081, and 1050788, the University of
33 Chile, and the Universidad Tecnológica Metropolitana and the EU-Network of Excellence P/hOREMOST
34 (FP6/2003/IST/2-511616) are also gratefully acknowledged.
35

36 References

- 37 [1] P. X. Gao, Z. L. Wang, *Appl. Phys. Lett.* **84**, 2883 (2004).
38 [2] N. Soga, M. Senna, *Sol. Stat. Ion.* **63-65**, 471 (1993).
39 [3] P. Gomez-Romero, *Adv. Mater.* **13**, 163 (2001).
40 [4] J. F. Xu, R. Czerw, S. Webster, D. L. Caroll, J. Ballato, R. Nesper, *Appl. Phys. Lett.* **79**, 1711 (2002).
41 [5] C. Gomez-Navarro, P. J. de Pablo, J. Colchero, Y. Fan, M. Burghard, J. Gomez-Herrero, A. M. Baro,
42 *Nanotechnology* **14**, 134 (2003).
43 [6] V. Lavayen, C. O'Dwyer, S. B. Newcomb, M. A. Santa Ana, E. Benavente, G. Gonzalez, C. M. Sotomayor
44 Torres, *phys. stat. sol. (b)* **243**, 3285 (2006).
45 [7] C. O'Dwyer, D. Navas, V. Lavayen, E. Benavente, M. A. Santa Ana, G. Gonzalez, S. B. Newcomb, C. M.
46 Sotomayor Torres, *Chem. Mater.* **18**, 3016 (2006).
47 [8] D. B. McWhan, M. Marezio, J. P. Remeika, P. D. Dernier, *Phys. Rev. B* **10**, 490 (1974).
48 [9] C. O'Dwyer, V. Lavayen, S. B. Newcomb, M. A. Santa Ana, E. Benavente, G. Gonzalez, C. M. Sotomayor
49 Torres, *Electrochem. Solid-State Lett.* **10**, A111 (2007).
50 [10] P. Tolédano and V. Dmitriev, *Reconstructive Phase Transitions* (World Scientific, Singapore, 1996).
51 [11] H. Katzke, P. Tolédano, W. Depmeier, *Phys. Rev. B* **68**, 024109 (2003).
52